Current Biology *16*, 2345–2351, December 5, 2006 ©2006 Elsevier Ltd All rights reserved DOI 10.1016/j.cub.2006.10.024

Report

Myosin-Va Facilitates the Accumulation of mRNA/Protein Complex in Dendritic Spines

Atsushi Yoshimura,[1,2] Ritsuko Fujii,[1] Yasuhito Watanabe,[1,3] Shigeo Okabe,[5] Kenji Fukui,[2] and Toru Takumi[1,4,*]

[1] Osaka Bioscience Institute
Suita, Osaka 565-0874
Japan

[2] Department of Psychiatry
Graduate School of Medical Sciences
Kyoto Prefectural University of Medicine
Kamigyo, Kyoto 602-8566
Japan

[3] Graduate School of Biostudies

[4] Graduate School of Medicine
Kyoto University
Sakyo, Kyoto 606-8501
Japan

[5] Department of Cell Biology
Tokyo Medical and Dental University Graduate School
Bunkyo, Tokyo 113-8519
Japan

Summary

mRNA localization has an essential role in localizing cytoplasmic determinants, controlling the direction of protein secretion, and allowing the local control of protein synthesis in neurons [1, 2]. In neuronal dendrites, the localization and translocation of mRNA is considered as one of the molecular bases of synaptic plasticity. Recent imaging and functional studies revealed that several RNA-binding proteins form a large messenger ribonucleoprotein (mRNP) complex that is involved in transport and translation of mRNA in dendrites [3, 4]. However, the mechanism of mRNA translocation into dendritic spines is unknown. Here, we show that an actin-based motor, myosin-Va [5, 6], plays a significant role in mRNP transport in neuronal dendrites and spines. Myosin-Va was Ca^{2+}-dependently associated with TLS, an RNA-binding protein, and its target RNA Nd1-L, an actin stabilizer. A dominant-negative mutant or RNAi of myosin-Va in neurons suppressed TLS accumulation in spines and further impaired TLS dynamics upon activation of mGluRs. The TLS translocation into spines was impeded also in neurons prepared from myosin-Va-null *dilute-lethal* (*dl*) mice, which exhibit neurological defects [7]. Our results demonstrate that myosin-Va facilitates the transport of TLS-containing mRNP complexes in spines and may function in synaptic plasticity through Ca^{2+} signaling.

Results and Discussion

TLS (translocated in liposarcoma) is colocalized with actin filaments in dendritic spines of hippocampal neurons [8, 9]. Proteomic studies revealed that TLS is included in an N-methyl-D-aspartate (NMDA) receptor complex [10] and in an RNA-transporting granule associated with conventional kinesin (KIF5) [11]. We previously reported that TLS binds to mRNA encoding an actin-stabilizing protein, Nd1-L, and is essential for normal spine development [12]. TLS is translocated into spines upon metabotropic glutamate receptor 5 (mGluR5) activation, and dendritic transport of TLS is dependent not only on microtubules but also on actin filaments [8]. To examine whether TLS interacts with myosin-Va, we performed immunoprecipitation (IP)-immunoblotting (IB) of mouse brain lysates with specific antibodies against TLS and myosin-Va. In the presence of EDTA and EGTA, TLS was coimmunoprecipitated with myosin-Va. However, no significant association of TLS with myosin-Va was observed in the presence of 100 μM $CaCl_2$ (Figure 1A). In addition to the ~190 kDa band expected, a ~130 kDa band was observed, and this probably represents a breakdown product of myosin-Va as previously described [13, 14]. This divalent cation-dependent dissociation was specific for Ca^{2+} because a strong or rather enhanced band was seen in the presence of 2.5 mM $MgCl_2$ (Figure 1B). Similar results were obtained from coimmunoprecipitation experiments in the reverse order (see Figure S1A in the Supplemental Data available with this article online). The conformation of myosin-V and its association with calmodulin (CaM) are regulated by Ca^{2+} concentration [15, 16]. Ca^{2+}/CaM-dependent protein kinase II (CaMKII) is a Ca^{2+}-stimulated enzyme that is abundant in the central nervous system and is one of the first CaM-regulated enzymes to be implicated in synaptic plasticity [17]. In the presence of two different CaMKII inhibitors, KN93 and AIP, the binding of myosin-Va with TLS was observed; however, the band was weaker compared with that in the presence of EDTA (Figure S1B). This result suggests that the CaMKII signaling is one of the pathways in this Ca^{2+} dependency, but there may exist other mechanisms. We then examined the dose dependency of the Ca^{2+} and Mg^{2+} ion effects. IP-IB experiments demonstrated that the binding affinity of TLS and myosin-Va decayed as the Ca^{2+} concentration was increased to 10–100 μM (Figure 1C), which is close to the Ca^{2+} concentration in spines after synaptic stimulation [18]. The interaction was reinforced as the Mg^{2+} concentration was increased from 2.5 μM to 2.5 mM (Figure 1D). This is in tune with a recent study that shows Mg^{2+} also regulating conformational changes in myosin-V [19].

We next performed subcellular fractionation of protein extracts from adult mouse brain cortex and hippocampus (Figure S2A). By using PSD95 as a marker for P2, GRP78 for P3, and P70 S6 kinase for supernatant fractions as controls, we found the intracellular distribution of myosin-Va to be similar to that of TLS (Figure S2B). The main difference was that myosin-Va is not detectable in the P1 nuclear fraction, whereas TLS was abundant in this fraction, as in previous reports [8, 11]. The

*Correspondence: takumi@obi.or.jp

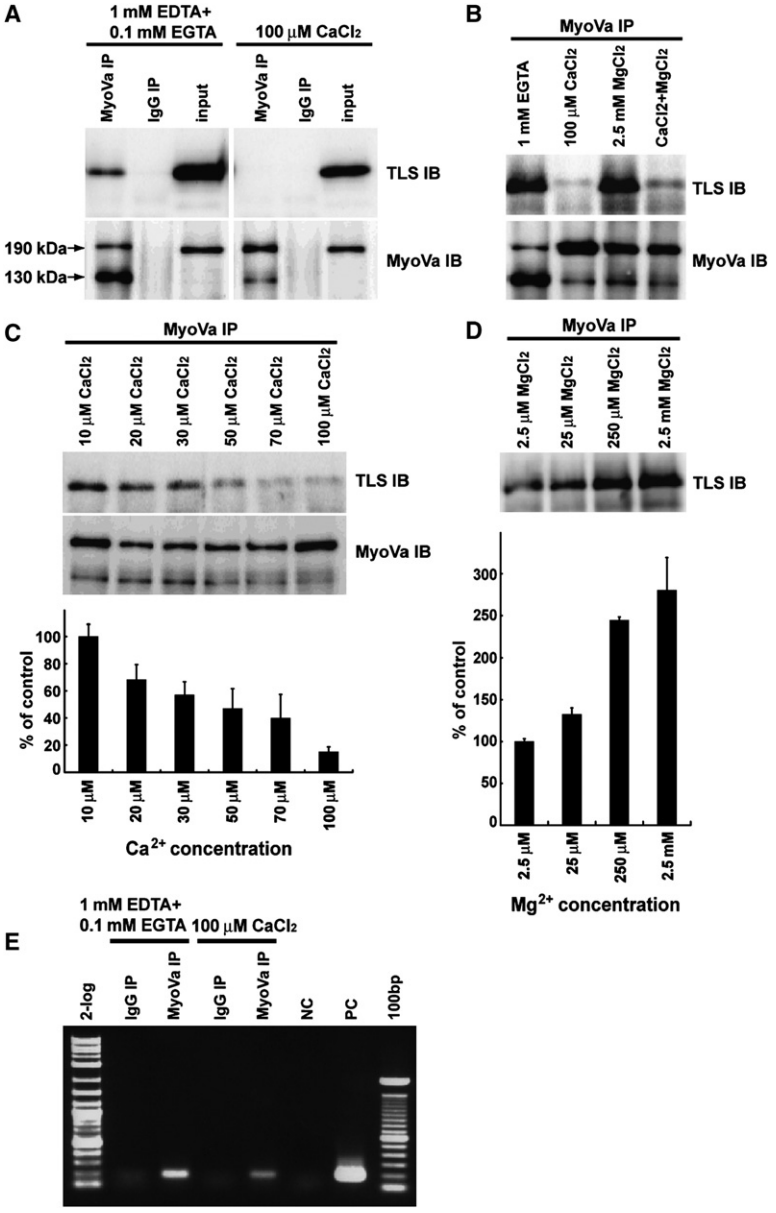

Figure 1. Interaction of Myosin-Va with TLS and Nd1-L mRNA

(A) Ca^{2+}-dependent binding of TLS to myosin-Va. Whole brain lysates from adult mice were subjected to analysis. TLS was coimmunoprecipitated with myosin-Va (MyoVa) by using myosin-Va antibody in the presence of chelating reagents but not in the presence of Ca^{2+}. Anti-rabbit IgG was used as a nonspecific binding control. One percent of the input used for immunoprecipitation was run in parallel.

(B) Interaction of TLS with MyoVa was detected in the presence of a chelator or Mg^{2+} but not in the presence of a high Ca^{2+} concentration (100 μM).

(C) Effects of Ca^{2+} concentration on TLS-MyoVa interaction. The TLS-MyoVa interaction was attenuated as Ca^{2+} concentration was increased to 100 μM. The amount of immunoprecipitates was quantified from luminescent images. Error bars represent SEM.

(D) Effects of Mg^{2+} concentration on TLS-MyoVa interaction. Mg^{2+}-dependent reinforcement of TLS-MyoVa interaction was observed in the range of 2.5 μM to 2.5 mM. Error bars represent SEM.

(E) IP/RT-PCR for detecting association of myosin-Va with Nd1-L mRNA. Myosin-Va was associated with Nd1-L mRNA, and the association seemed to be Ca^{2+} dependent. NC stands for no template for PCR; PC stands for mouse brain cDNA being used as a template. 2-log, 2-log DNA ladder; 100 bp, 100 bp DNA ladder.

IP-IB experiments exhibited interaction of TLS with myosin-Va in the P3 polysome extract (Figure S2C). Furthermore, IP-IB experiments with neuronal PC12 cells also revealed an association of myosin-Va with TLS. However, overexpression experiments for myosin-Va and TLS in nonneuronal HEK293T cells did not show their binding (data not shown), suggesting that formation of the myosin-Va-TLS complex may require other neuron-specific proteins.

To see whether myosin-Va forms a complex with a specific TLS target, Nd1-L mRNA [12], we performed IP/RT-PCR. We used anti-myosin-Va antibody to immunoprecipitate a myosin-Va complex from mouse brain. Immunoprecipitaed RNAs were reverse transcribed with random hexamer. The resulting cDNAs were subjected to PCR with specific primers for Nd1-L mRNA. The amplified PCR products for Nd1-L mRNA migrated to the same position as the control cDNA products obtained from mouse brain RNA (Figure 1E). The band in the presence of EDTA and EGTA was stronger than that in 100 μM $CaCl_2$. As a control, tubulin β3 mRNA was not detected as clearly as the case of Nd1-L (Figure S1C). These data demonstrate that in the myosin-Va immunoprecipitates, Nd1-L mRNA localization is also regulated by Ca^{2+}, and such finding is consistent with the above TLS results.

To test whether myosin-Va plays a role in the transport of TLS into dendritic spines, we analyzed the localization of GFP- or red fluorescent protein (RFP)-tagged TLS (TLS-GFP or TLS-RFP) in cultured mouse hippocampal neurons together with that of full-length myosin-Va (BRMV) or three kinds of tail domains of its brain-specific isoforms, i.e., brain short tail (BRST), brain stalk (BRSTK), and globular tail domain (GTD) [20]. The tail domain is thought to be involved in cargo binding [5, 6], and the mutation in this region causes the Griscelli syndrome [21]. As reported previously [8], TLS-GFP exhibited a punctate distribution in dendrites and was localized in

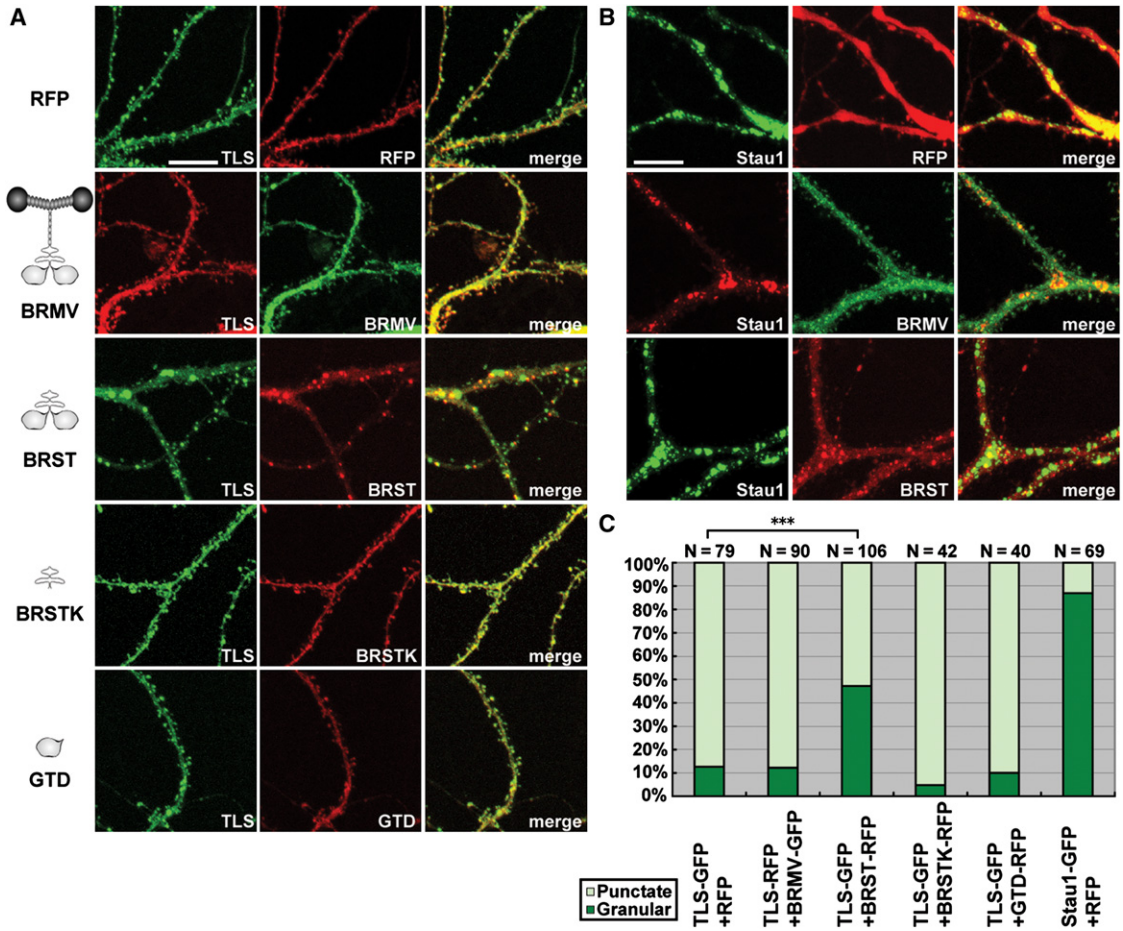

Figure 2. Suppression of Translocation of TLS into Dendritic Spines by Dominant-Negative Myosin-Va Tail Domain

(A) Effect of the dominant-negative myosin-Va tail domain on localization of TLS in mouse hippocampal neurons. TLS-GFP was diffusely distributed in somatodendritic domains and was accumulated at spines in control medium. The translocation of TLS-GFP into spines was suppressed by overexpression of BRST-RFP. The other myosin-Va tail domains (BRSTK and GTD) and full-length myosin-Va (BRMV) did not affect translocation of TLS-GFP (RFP). Each image is a 2D projection of a 3D stack of 5–7 z sections, each of 0.5 μm thickness. The scale bar represents 10 μm.

(B) Staufen1-GFP (RFP) exhibited granular expression pattern and was localized in dendritic shafts. Its pattern was not affected by full-length myosin-Va (BRMV) or by dominant-negative myosin-Va tail domain (BRST). The scale bar represents 10 μm.

(C) The distributions of fluorescent proteins fused to TLS were classified as two patterns: a granular pattern, with clusters predominantly found in dendritic shafts, and a punctate pattern, with the proteins diffusely distributed in somatodendritic domains and accumulated in dendritic spines. The percentage of either pattern under each experimental condition was calculated. ***$p < 0.0001$; test for equal proportions.

spines, and this type is called "Punctate" (Figure 2A, RFP). The TLS-RFP particles were colocalized with GFP-tagged myosin-Va (BRMV-GFP), particularly in spines (Figure 2A, BRMV). Whereas BRSTK-RFP and GTD-RFP did not affect the localization of TLS-GFP (Figure 2A, BRSTK and GTD), overexpression of BRST-RFP, containing both medial tail (stalk) and globular tail domains of myosin-Va, inhibited the translocation of TLS-GFP into spines and resulted in a granular expression pattern within the dendrites, and this type is called "Granular" (Figure 2A, BRST). The diffuse distribution of GFP in neurons was not affected by BRST-RFP (data not shown). A quantitative analysis revealed that the granular type of TLS-GFP (RFP) that clusters within dendritic shafts was observed in approximately 50% of neurons cotransfected with BRST-RFP, whereas that these granular clusters were found in only about 10% of neurons with RFP, BRMV-GFP, BRSTK-RFP, or GTD-RFP ($p < 0.0001$), with the rest of them (~90%) exhibiting the punctate-type distribution (Figure 2C). Consistent with these imaging data, biochemical experiments showed that only the BRST interacted with TLS among these mutants and that endogenous full-length myosin-Va was associated with BRST-FLAG in PC12 cells (Figure S3), indicating that BRST dimerized with an endogenous myosin-Va heavy chain. These results suggest that BRST functions as a dominant-negative mutant and that transport of TLS into spines is interfered by BRST.

Different from TLS, Staufen, another RNA-binding protein and a constituent of RNA granules in mammalian neurons [11, 22–24], is recruited to dendrites via a microtubule system, but not by actin filaments [8, 25]. Coimmunoprecipitation experiments revealed that Staufen did not bind with myosin-Va in mouse brain lysates even in the presence of Ca^{2+} chelators (data not shown). In cultured hippocampal neurons, GFP-fused Staufen1 (Stau1-GFP) exhibited the granular expression pattern,

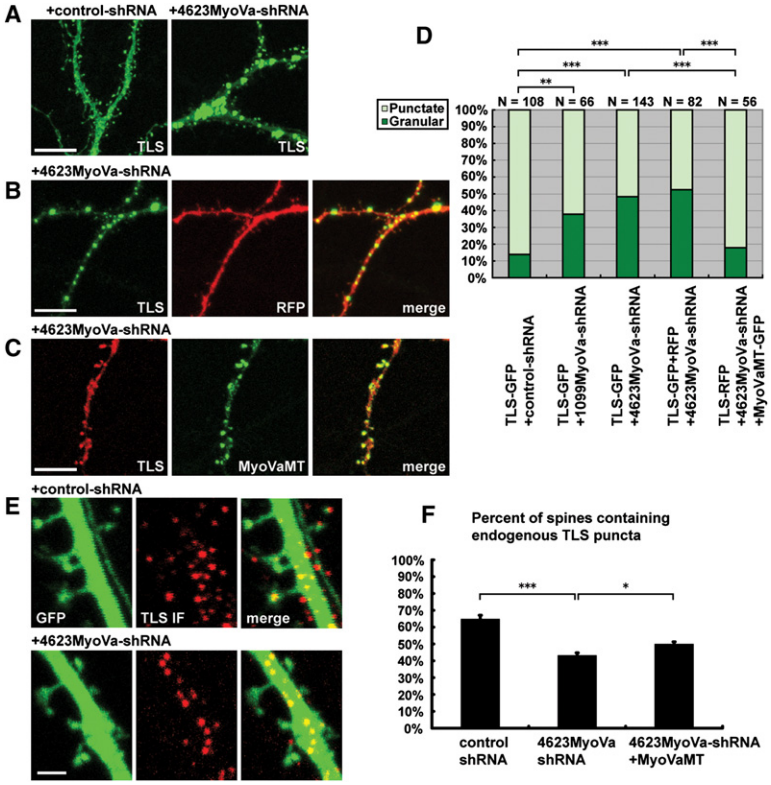

Figure 3. Impairment of TLS Accumulation into Dendritic Spines by Myosin-Va Silencing

(A) Translocation of TLS into dendritic spines was repressed in myosin-Va-shRNA-treated neurons. TLS-GFP and shRNA vectors were microinjected into the nucleus of hippocampal neurons. Forty-eight hours after the microinjection, the neurons were fixed and the distributions of TLS-GFP were compared for the different experimental conditions. The scale bar represents 10 μm.

(B) TLS-GFP stayed within the dendritic shafts after myosin-Va silencing. TLS-GFP, 4623MyoVa-shRNA, and RFP vectors were introduced into hippocampal neurons. The scale bar represents 10 μm.

(C) TLS accumulation in dendritic spines was restored through MyoVaMT constructs, in neurons treated with 4623MyoVa-shRNA. The domain targeted by 4623MyoVa-shRNA is mutated in MyoVaMT constructs. The scale bar represents 10 μm.

(D) The distribution patterns of TLS-GFP were counted under each condition. The reduction of TLS accumulation into spines in 4623MyoVa-shRNA coinjected populations was resolved by MyoVaMT constructs. **p = 0.0003, ***p < 0.0001; test for equal proportions.

(E) Endogenous TLS was localized in dendritic spines in control-shRNA-treated neurons. Such localization was absent in 4623MyoVa-shRNA-treated neurons. The scale bar represents 2 μm.

(F) Analysis of endogenous TLS puncta in dendritic spine head areas (control, n = 11 cells; 4623MyoVa-shRNA, n = 21 cells; 4623MyoVa-shRNA^{+}MyoVaMT, n = 13 cells from two independent experiments). Error bars represent SEM. *p = 0.003, ***p < 0.0001; ANOVA test.

consistent with previous reports [23, 25], and was not present in dendritic spines (Figures 2B and 2C). The localization of Stau1 fused with fluorescent proteins was not affected by BRMV-GFP or BRST-RFP (Figure 2B). Taken together with results on TLS, these findings suggest that the interaction of RNA-binding proteins with myosin-Va is required for their translocation into spines.

To clarify whether the endogenous myosin-Va plays a critical role in the transport of RNA-binding proteins into spines, we adopted RNA interference (RNAi) technique. We introduced myosin-Va or control-short hairpin (sh)RNA together with TLS-GFP by microinjection into the nucleus of primary hippocampal neurons. In neurons expressing control-shRNA, TLS-GFP accumulated in dendritic spines (~90%, Figure 3A, left and Figure 3D). In about 50% of the neurons challenged by 4623MyoVa-shRNA with or without RFP, TLS-GFP formed dense clusters in dendritic shafts ($p < 0.0001$; Figure 3A, right and Figures 3B and 3D), as observed in neurons expressing the dominant-negative myosin-Va tail domain (Figures 2A and 2C). Coinjection of another RNAi construct, 1099MyoVa-shRNA, led to more than a 35% increase in the number of granular-type clusters of TLS-GFP, and such increase was statistically significant compared with the control ($p < 0.001$; Figure 3D). Specific myosin-Va knockdown was confirmed by western blotting, fluorescence intensity, and immunocytochemistry (Figure S4A–S4D). Next, as a rescue control, we constructed MyoVaMT, a full-length version of myosin-Va containing silent nucleotide changes that render it impervious to 4623MyoVa-shRNA. The expression of MyoVaMT against shRNAs was also verified by western blotting (Figure S4E). In neurons expressing 4623MyoVa-shRNA together with MyoVaMT, the localization of TLS into dendritic spines was observed and the percentage of punctate-type expression of TLS-GFP increased to more than 80% (Figure 3C; $p < 0.0001$, Figure 3D). We further examined whether endogenous TLS showed a similar redistribution under different conditions. Immunostaining with TLS polyclonal antibody (TLS-C) exhibited a punctate distribution within dendrites (Figure S5A) as described previously [8]. In neurons expressing control-shRNA, ~70% of spines contained endogenous TLS puncta, whereas ~40% of spines showed TLS-positive immunolabeling in neurons expressing 4623MyoVa-shRNA (Figures 3E and 3F; $p < 0.0001$). In neurons challenged by MyoVaMT in addition to 4623MyoVa-shRNA, TLS-positive spines were restored to ~50% compared with neurons expressing 4623MyoVa-shRNA (Figure 3F and Figure S5B; $p = 0.003$). Taken together, endogenous myosin-Va knockdown, which was achieved by two different shRNAs, resulted in inhibition of translocation of TLS into spines.

Local protein synthesis subsequent to translocation of mRNA to dendrites is known to be stimulated by DHPG, a group 1 mGluR agonist [26]. To investigate how TLS dynamics would be affected by the loss-of-function of myosin-Va, we stimulated cultured hippocampal neurons expressing TLS-GFP with 100 μM DHPG over 60 min and monitored the movement of TLS-GFP by time-lapse confocal microscopy (Movie S1). The TLS-GFP particles were translocated into spines (Figure S6A,

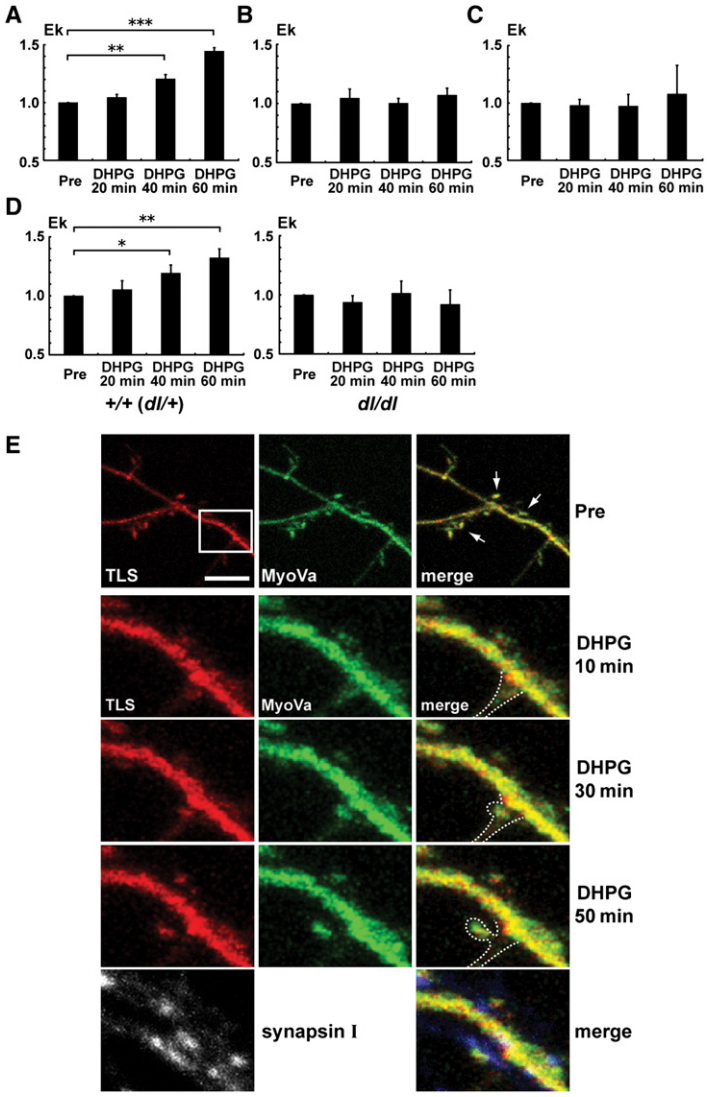

Figure 4. Myosin-Va and TLS Dynamics in Dendritic Spines

(A) Histograms showing enrichment of TLS in dendritic spines after DHPG stimulation. The relative enrichment at the indicated time span of TLS-GFP in spines (Ek) was calculated from the averaged fluorescence intensity in spines and the underlying dendritic shaft during 20 min before and after DHPG stimulation. Error bars represent SEM. **p = 0.0005, ***p < 0.0001; ANOVA test.

(B) Quantification of enrichment of TLS-GFP in dendritic spines under the overexpression of BRST-RFP. There was no significant difference before and after DHPG treatment. Error bars represent SEM.

(C) Quantification of enrichment of TLS-GFP into dendritic spines under silencing of myosin-Va by 4623MyoVa-shRNA. There was no significant difference before and after the DHPG treatment. Error bars represent SEM.

(D) The gradual enrichment of TLS-GFP in dendritic spines was observed in neurons of +/+ (and *dl*/+) mice. No enrichment was observed in neurons of *dilute-lethal dl/dl* mice. Error bars represent SEM. *p < 0.02, **p < 0.0003; ANOVA test.

(E) Two-color real-time imaging of TLS-RFP and MyoVa-GFP showed that both two moved together into the same protrusion extended from dendritic shaft after DHPG treatment. The protrusion presented spine morphology and retrospective immunostaining with anti-synapsin I revealed that the spine formed the synapse. Images presented are projections assembled from confocal optical sections at the indicated time. Lower panels show enlarged images of the white rectangular area shown in an upper left panel. Dashed lines indicate the putative outline of the dendrite. The scale bar represents 5 μm.

inset), and the fluorescence intensity of TLS-GFP in spines was gradually enhanced (Figure S7A) as we have previously reported [8]. The dendritic spines were confirmed by retrospective immunocytochemistry with synapsin I antibody, and this revealed the presence of their presynaptic component (Figure S6A). The relative enrichment at the indicated time span (Ek) of TLS-GFP in spines was significantly increased after mGluR stimulation (Figure 4A; $p < 0.0005$ for 40 min, $p < 0.0001$ for 60 min). On the contrary, in neurons expressing the dominant-negative myosin-Va tail domain (BRST-RFP), TLS-GFP clusters were localized in dendritic shafts (Figure S6B), and the intensity of TLS-GFP in the spines remained low even after synaptic stimulation with DHPG (Figure 4B and Figure S7B). In myosin-Va-knockdown neurons obtained by injection of 4623MyoVa-shRNA, the TLS-GFP clusters formed granules and were located within the dendritic shafts (Figure S6C). The intensity of TLS-GFP in spines exhibited larger fluctuations than in control neurons. Nevertheless, the translocation of TLS-GFP in spines was impaired by knocking down myosin-Va expression (Figure 4C and Figure S7C). To ascertain the effects of myosin-Va on spine morphology, we introduced BRST-RFP and 4623MyoVa-shRNA by microinjection into the nucleus of cultured hippocampal neurons along with a GFP vector, which outlined the morphology of the injected neurons. Compared with the spines in neurons expressing GFP alone, some spines in the neurons coexpressing GFP+BRST or GFP+4623MyoVa-shRNA tended to be thinner and longer (Figure S4D, arrows). In cumulative-frequency plots, although knockdown of myosin-Va induced a slight rightward shift in spine length and a little leftward shift in spine head diameter (Figures S8A, S8B, and S8D), the difference in the spine head area was negligible (Figures S8C and S8D). These results indicate that the transport of TLS-GFP into spines was suppressed by knockdown of myosin-Va and that myosin-Va has likely been involved in the translocation of RNA-binding proteins such as TLS into spines.

We further verified the results of the above knockdown experiments by using neurons derived from myosin-Va-deficient *dilute-lethal* (*dl/dl*) mice [7]. The distribution of TLS-GFP was investigated in myosin-Va null *dl/dl* neurons and +/+ (and hetrozygotes *dl*/+). TLS-GFP was clustered within dendritic shafts in some

dl/*dl* neurons (Figure S9A) as was observed in neurons expressing the dominant-negative myosin-Va tail domain or myosin-Va-shRNA (Figures 2A, 3A, and 3B). The average ratio of *dl*/*dl* neurons with a granular pattern was ~30%, clearly higher than that of control neurons (<~10%), as seen in the experiments using the dominant-negative and shRNA ($p < 0.01$, Figures 2C and 3D), whereas the difference compared with that for +/+ (and *dl*/+) neurons did not reach a statistically significant level ($p = 0.0874$, Figure S9B). This was probably because +/+ neurons in our specimens may have included *dl*/+ neurons owing to the difficulty in strict discrimination between +/+ and *dl*/+ neurons by genotyping based on the quantity available for immunoblotting and immunocytochemistry. The time-lapse imaging experiments substantiated this assumption and demonstrated that DHPG stimulation induced TLS-GFP enrichment in spines of +/+ (and *dl*/+) neurons, whereas the induction was impaired in *dl*/*dl* neurons (Figure 4D). These data corroborate our other data showing that myosin-Va played a pivotal role in TLS translocation into dendritic spines and that its dysfunction may account for the mechanism of neurological defects in *dilute-lethal* mice [7] and human Griscelli syndrome [21]. The neurological defects in *dilute-lethal* mice are now known [27]. For example, long-term synaptic depression (LTD) is abolished in *dilute-lethal* mice [28], in which Purkinje cells lack smooth endoplasmic reticulum (SER) in spines [29]. The transport of RNA granules and SER may be reciprocally interacted through myosin-Va.

To provide direct evidence that myosin-Va is involved in the localization of a TLS-containing particle into dendritic spines, we performed two-color real-time imaging. Neurons expressing TLS-RFP and MyoVa-GFP were treated with DHPG 24 hr after microinjection and were monitored by time-lapse confocal microscopy (Figure 4E and Movie S2). Some TLS-RFP had already been accumulated in spines with MyoVa-GFP before DHPG treatment (Figure 4E, upper panels, arrows; also see Figure 2A, BRMV). A protrusion from a dendritic shaft emerged after DHPG treatment, as expected from the previous report [30]. TLS-RFP and MyoVa-GFP moved together into the extending protrusion, which represented spine morphology (Figure 4E, lower panels). The protrusion formed a synapse, which was verified by retrospective immunostaining by anti-synapsin I. The data in Figure 4E is consistent with the idea that myosin-Va translocates the TLS-containing RNA particles into spines.

Our present model proposes that a subset of RNA granules including RNA-binding proteins such as TLS is transported in a short-range manner into dendritic spines by myosin-Va (Figure S10). RNA granules including RNA-binding proteins with their target mRNAs are delivered within dendrites in a long-range fashion by microtubule-dependent motors such as KIF5 [11, 31], acting coordinately with myosin-V [32]. At the local area or spines where mRNAs can be translated upon synaptic stimulation [33], some components including "TLS-type" RNA-binding proteins dissociate from the core RNA granules and translocate into dendritic spines. On the other hand, other components including "Staufen-type" RNA-binding proteins stay within the dendritic shafts. Recent studies show that the actin-binding affinity of myosin-V is reduced, and its transport velocity along actin filaments becomes slower as the Ca^{2+} concentration increases [15, 16]. Thus, myosin-Va interacts with TLS and transports its bound mRNAs such as Nd1-L into dendritic spines [12], where myosin-Va releases TLS and its bound mRNAs for local translation upon Ca^{2+} influx through NMDA receptors and voltage-gated Ca^{2+} channels [4]. The mechanism may include tail phosphorylation of myosin-V by calcium/calmodulin-dependent protein kinase II (CaMKII) as observed in *Xenopus* melanophores [34]. Our present findings provide not only the mechanism by which myosin-Va may be involved in mRNA transport into postsynaptic spines but also compelling evidence that myosin-based mRNA and organelle transport systems emerged in unicellular eukaryotes and have been widely used throughout evolution [35].

Supplemental Data

Supplemental Data include Experimental Procedures, ten figures, and two movies and can be found with this article online at http://www.current-biology.com/cgi/content/full/16/23/2345/DC1/.

Acknowledgments

We thank S. Tsuboi, Y. Shima, T. Sudo, and D. Saito for their technical assistance and Y. Takagishi and S. Oda for technical comments. We are grateful to S. Nakanishi, H. Sabe, and J. Myung for their critical comments on this manuscript and J. Hammer III, N. Hirokawa, M. Kiebler, R. Tsien, T. Kono, and N. Jenkins for providing reagents and information. This work was supported in part by research grants from the Japan Ministry of Education, Culture, Sports, Science, and Technology, the Mitsubishi Pharma Research Foundation, the NOVARTIS Foundation (Japan) for the Promotion of Science, and Sony Corporation.

Received: April 7, 2006
Revised: September 17, 2006
Accepted: October 5, 2006
Published: December 4, 2006

References

1. Jansen, R.P. (2001). mRNA localization: Message on the move. Nat. Rev. Mol. Cell Biol. *2*, 247–256.
2. St Johnston, D. (2005). Moving messages: The intracellular localization of mRNAs. Nat. Rev. Mol. Cell Biol. *6*, 363–375.
3. Bagni, C., and Greenough, W.T. (2005). From mRNP trafficking to spine dysmorphogenesis: The roots of fragile X syndrome. Nat. Rev. Neurosci. *6*, 376–387.
4. Steward, O., and Schuman, E.M. (2003). Compartmentalized synthesis and degradation of proteins in neurons. Neuron *40*, 347–359.
5. Langford, G.M. (2002). Myosin-V, a versatile motor for short-range vesicle transport. Traffic *3*, 859–865.
6. Reck-Peterson, S.L., Provance, D.W., Jr., Mooseker, M.S., and Mercer, J.A. (2000). Class V myosins. Biochim. Biophys. Acta *1496*, 36–51.
7. Mercer, J.A., Seperack, P.K., Strobel, M.C., Copeland, N.G., and Jenkins, N.A. (1991). Novel myosin heavy chain encoded by murine dilute coat colour locus. Nature *349*, 709–713.
8. Fujii, R., Okabe, S., Urushido, T., Inoue, K., Yoshimura, A., Tachibana, T., Nishikawa, T., Hicks, G.G., and Takumi, T. (2005). The RNA binding protein TLS is translocated to dendritic spines by mGluR5 activation and regulates spine morphology. Curr. Biol. *15*, 587–593.
9. Belly, A., Moreau-Gachelin, F., Sadoul, R., and Goldberg, Y. (2005). Delocalization of the multifunctional RNA splicing factor TLS/FUS in hippocampal neurones: Exclusion from the nucleus and accumulation in dendritic granules and spine heads. Neurosci. Lett. *379*, 152–157.

10. Husi, H., Ward, M.A., Choudhary, J.S., Blackstock, W.P., and Grant, S.G. (2000). Proteomic analysis of NMDA receptor-adhesion protein signaling complexes. Nat. Neurosci. *3*, 661–669.
11. Kanai, Y., Dohmae, N., and Hirokawa, N. (2004). Kinesin transports RNA: Isolation and characterization of an RNA-transporting granule. Neuron *43*, 513–525.
12. Fujii, R., and Takumi, T. (2005). TLS facilitates transport of mRNA encoding an actin-stabilizing protein to dendritic spines. J. Cell Sci. *118*, 5755–5765.
13. Jung, C., Chylinski, T.M., Pimenta, A., Ortiz, D., and Shea, T.B. (2004). Neurofilament transport is dependent on actin and myosin. J. Neurosci. *24*, 9486–9496.
14. Watanabe, M., Nomura, K., Ohyama, A., Ishikawa, R., Komiya, Y., Hosaka, K., Yamauchi, E., Taniguchi, H., Sasakawa, N., Kumakura, K., et al. (2005). Myosin-Va regulates exocytosis through the submicromolar Ca2+-dependent binding of syntaxin-1A. Mol. Biol. Cell *16*, 4519–4530.
15. Krementsov, D.N., Krementsova, E.B., and Trybus, K.M. (2004). Myosin V: Regulation by calcium, calmodulin, and the tail domain. J. Cell Biol. *164*, 877–886.
16. Nguyen, H., and Higuchi, H. (2005). Motility of myosin V regulated by the dissociation of single calmodulin. Nat. Struct. Mol. Biol. *12*, 127–132.
17. Xia, Z., and Storm, D.R. (2005). The role of calmodulin as a signal integrator for synaptic plasticity. Nat. Rev. Neurosci. *6*, 267–276.
18. Segal, M. (2005). Dendritic spines and long-term plasticity. Nat. Rev. Neurosci. *6*, 277–284.
19. Rosenfeld, S.S., Houdusse, A., and Sweeney, H.L. (2005). Magnesium regulates ADP dissociation from myosin V. J. Biol. Chem. *280*, 6072–6079.
20. Wu, X., Wang, F., Rao, K., Sellers, J.R., and Hammer, J.A., 3rd. (2002). Rab27a is an essential component of melanosome receptor for myosin Va. Mol. Biol. Cell *13*, 1735–1749.
21. Pastural, E., Barrat, F.J., Dufourcq-Lagelouse, R., Certain, S., Sanal, O., Jabado, N., Seger, R., Griscelli, C., Fischer, A., and de Saint Basile, G. (1997). Griscelli disease maps to chromosome 15q21 and is associated with mutations in the myosin-Va gene. Nat. Genet. *16*, 289–292.
22. Kiebler, M.A., Hemraj, I., Verkade, P., Kohrmann, M., Fortes, P., Marion, R.M., Ortin, J., and Dotti, C.G. (1999). The mammalian staufen protein localizes to the somatodendritic domain of cultured hippocampal neurons: Implications for its involvement in mRNA transport. J. Neurosci. *19*, 288–297.
23. Kohrmann, M., Luo, M., Kaether, C., DesGroseillers, L., Dotti, C.G., and Kiebler, M.A. (1999). Microtubule-dependent recruitment of Staufen-green fluorescent protein into large RNA-containing granules and subsequent dendritic transport in living hippocampal neurons. Mol. Biol. Cell *10*, 2945–2953.
24. Ohashi, S., Koike, K., Omori, A., Ichinose, S., Ohara, S., Kobayashi, S., Sato, T.A., and Anzai, K. (2002). Identification of mRNA/protein (mRNP) complexes containing Puralpha, mStaufen, fragile X protein, and myosin Va and their association with rough endoplasmic reticulum equipped with a kinesin motor. J. Biol. Chem. *277*, 37804–37810.
25. Tang, S.J., Meulemans, D., Vazquez, L., Colaco, N., and Schuman, E. (2001). A role for a rat homolog of staufen in the transport of RNA to neuronal dendrites. Neuron *32*, 463–475.
26. Job, C., and Eberwine, J. (2001). Localization and translation of mRNA in dendrites and axons. Nat. Rev. Neurosci. *2*, 889–898.
27. Bridgman, P.C. (2004). Myosin-dependent transport in neurons. J. Neurobiol. *58*, 164–174.
28. Miyata, M., Finch, E.A., Khiroug, L., Hashimoto, K., Hayasaka, S., Oda, S.I., Inouye, M., Takagishi, Y., Augustine, G.J., and Kano, M. (2000). Local calcium release in dendritic spines required for long-term synaptic depression. Neuron *28*, 233–244.
29. Takagishi, Y., Oda, S., Hayasaka, S., Dekker-Ohno, K., Shikata, T., Inouye, M., and Yamamura, H. (1996). The dilute-lethal (dl) gene attacks a Ca2+ store in the dendritic spine of Purkinje cells in mice. Neurosci. Lett. *215*, 169–172.
30. Vanderklish, P.W., and Edelman, G.M. (2002). Dendritic spines elongate after stimulation of group 1 metabotropic glutamate receptors in cultured hippocampal neurons. Proc. Natl. Acad. Sci. USA *99*, 1639–1644.
31. Knowles, R.B., Sabry, J.H., Martone, M.E., Deerinck, T.J., Ellisman, M.H., Bassell, G.J., and Kosik, K.S. (1996). Translocation of RNA granules in living neurons. J. Neurosci. *16*, 7812–7820.
32. Huang, J.D., Brady, S.T., Richards, B.W., Stenolen, D., Resau, J.H., Copeland, N.G., and Jenkins, N.A. (1999). Direct interaction of microtubule- and actin-based transport motors. Nature *397*, 267–270.
33. Ostroff, L.E., Fiala, J.C., Allwardt, B., and Harris, K.M. (2002). Polyribosomes redistribute from dendritic shafts into spines with enlarged synapses during LTP in developing rat hippocampal slices. Neuron *35*, 535–545.
34. Karcher, R.L., Roland, J.T., Zappacosta, F., Huddleston, M.J., Annan, R.S., Carr, S.A., and Gelfand, V.I. (2001). Cell cycle regulation of myosin-V by calcium/calmodulin-dependent protein kinase II. Science *293*, 1317–1320.
35. Vale, R.D. (2003). The molecular motor toolbox for intracellular transport. Cell *112*, 467–480.